# Emergent dynamics of a three-node regulatory network explain phenotypic switching and heterogeneity during helper T-cell differentiation

Running title: T-bet/GATA3/RORγT network dynamics regulate phenotypic switching

Atchuta Srinivas Duddu[1], Siddharth Jhunjhunwala[1], Mohit Kumar Jolly[1,*]

[1] Centre for BioSystems Science and Engineering, Indian Institute of Science, Bangalore, India

*Author to whom correspondence to be addressed: mkjolly@iisc.ac.in (M.K.J.)

**Abstract**

Naïve helper (CD4+) T-cells can differentiate into distinct functional subsets including Th1, Th2, and Th17 phenotypes. Each of these phenotypes has a 'master regulator' – T-bet (Th1), GATA3 (Th2) and RORγT (Th17) – that inhibits the other two master regulators. Such mutual repression among them at a transcriptional level can enable multistability, thus enabling the co-existence of six experimentally observed phenotypes – Th1, Th2, Th17 and hybrid Th/Th2, Th2/Th17 and Th1/Th17. However, the dynamics of switching among these phenotypes, particularly in the case of epigenetic influence, remains unclear. Here, through mathematical modeling, we investigated the coupled transcription-epigenetic network dynamics to elucidate how epigenetic changes mediated by these 'master regulators' can influence the transition rates among these different phenotypes. Further, we show that the degree of plasticity exhibited by one phenotype depends on relative strength and duration of mutual epigenetic repression mediated among the master regulators. Our model simulations possibly explain the relatively higher plasticity of Th17 phenotype as noticed *in vitro* and *in vivo*. Together, our modeling framework characterizes phenotypic plasticity and heterogeneity in a naïve helper (CD4+) T-cell population as an outcome of the emergent dynamics of a three node regulatory network, such as the one mediated by T-bet/GATA3/RORγT.

**Keywords**

Multistability, Phenotypic plasticity, T-cell differentiation, Epigenetic feedback, T-bet, GATA3, RORγT

## Introduction

Differentiation of naïve CD4+ T-cells into diverse T-helper (Th) cells facilitates versatile and adaptable immune responses to different challenges, and serves as a powerful model system to investigate cell-fate decision-making (Evans and Jenner, 2013). Different Th cells – Th1, Th2, Th17 among others – have distinct cytokine and functional profiles. Th1 cells mainly produce IFNγ, and mediate host defense against intracellular bacteria and viruses, while Th2 cells produce IL-4 and are implicated in allergic immune responses. Th17 cells secrete IL-17A, IL-17F and GM-CSF, and act against bacterial and fungal pathogens such as *Mycobacterium* (Kaiko *et al.*, 2008; Stadhouders *et al.*, 2018). Earlier thought to be mutually exclusive and (terminally) stable phenotypes, recent single-cell evidence has revealed the heterogeneity and plasticity of Th cell subsets. For instance, hybrid Th1/Th2, Th2/Th17 and Th1/Th17 phenotypes have been observed at a single-cell level *in vitro* and *in vivo* (Peine *et al.*, 2013; Chatterjee *et al.*, 2018; Xhangholi *et al.*, 2019; Tortola *et al.*, 2020). Moreover, *in vitro* restimulation can drive switching among multiple phenotypes – Th1, Th2, Th17 and the corresponding hybrid ones (Curtis *et al.*, 2010; Evans and Jenner, 2013; Tortola *et al.*, 2020; Cerboni *et al.*, 2021). However, a dynamical characterization of phenotypic switching among these Th cell subpopulations has not been performed.

T-bet, GATA3 and RORγT have been proposed as the 'master regulators' of Th1, Th2 and Th17 cells respectively. They can mutually repress each other and self-activate directly or indirectly, thus driving CD4+ naïve cell differentiation into diverse Th subsets (Fang and Zhu, 2017). Such mutual repression is a hallmark of 'sibling' cell-fates in many systems, such as for PU.1/GATA1 in the case of common myeloid progenitor differentiating to a myeloid or erythroid fate (Zhou and Huang, 2011), or ZEB1/GRHL2 for epithelial-mesenchymal transition (Hari *et al.*, 2020). Similar to PU.1/GATA1 and ZEB1/GRHL2, the T-bet/GATA3/RORγT regulatory network can be multistable, enabling the co-existence of different phenotypes and switching among them – Th1 (high T-bet, low GATA3, low RORγT), Th2 (low T-bet, high GATA3, low RORγT), Th17 (low T-bet, low GATA3, high RORγT), hybrid Th1/Th2 (high T-bet, high GATA3, low RORγT), hybrid Th2/Th17 (low T-bet, high GATA3, high RORγT) and hybrid Th1/Th17 (high T-bet, low GATA3, high RORγT). Intriguingly, self-activation of 'master regulators' can enrich for hybrid phenotypes (Duddu *et al.*, 2020). However, a comprehensive analysis of the interplay among factors influencing the rates of transition among these phenotypes remains to be done.

Epigenetic changes, including modifications of histones and DNA methylation status, can control the rate of phenotypic switching by influencing the access of 'master regulators' to their genome-wide targets. Thus, cell-specific chromatin landscape and 'histone code' can form stable epigenetic marks at various gene loci, thus governing the commitment, heritability and plasticity of various cell-fates (Chang and Aune, 2007; Miyamoto *et al.*, 2015; Suelves *et al.*, 2016). Early biochemical evidence for the importance of epigenetic processes in T-cell differentiation came from studies showing that treatment of T cells with inhibitors of histone deacetylases (HDACs) or DNA methylation led to the production of IL-2 and IFNγ by cells that could not previously produce them (Wilson *et al.*, 2009). Further, T-bet, GATA3 and RORγT have been shown to control chromatin accessibility required for T-cell differentiation into different lineages/phenotypes (Sanders, 2006; Hirahara *et al.*, 2011). Interestingly, such influence was shown to be at least partly independent of signals from cytokine receptors/signaling, suggesting many parallel paths that these 'master regulators' can take to suppress other lineages and to promote theirs (Josefowicz, 2013; Lee *et al.*, 2020). Such antagonism at both transcriptional and epigenetic levels have been witnessed in other instances of cell-fate decisions too (Tripathi *et al.*, 2020; Serresi *et al.*, 2021). Despite such wealth of molecular and functional data for T-cell differentiation, we are lacking a quantitative systems-level investigation how

the rates of phenotypic switching among Th1, Th2 and Th17 depend on the epigenetic influences mediated by T-bet, GATA3 and RORγT on the function of each other.

Here, we identify the emergent dynamics of a three-node system repressing each other at both transcriptional and epigenetic levels, using a mathematical modeling approach. Our simulations reveal that phenotypic plasticity and heterogeneity are governed by emergent dynamics of the 'toggle triad' network, such as the one formed by T-bet, GATA3 and RORγT. Rate of switching among phenotypes and consequent changes in population distribution of T-cell phenotypes is a function of relative strength and duration corresponding to epigenetic repression mediated by 'master regulators' on one another. The stronger the incoming epigenetic repression for a given master regulator, the higher the probability of switching out of the corresponding phenotype. Our results unravel a potential design principle of T-cell differentiation at individual cell and population levels.

## Results

### Relative abundance of T-bet, GATA3 and RORγT governs phenotypic heterogeneity in a T-cell population

The emergent dynamics of a network comprising two nodes repressing each other (toggle switch) have been extensively investigated both experimental and theoretically in diverse biological systems (Cherry and Adler, 2000; Gardner *et al.*, 2000; Graham *et al.*, 2010). A toggle switch explains the behavior of a progenitor cell differentiating into one of the two cell fates, each fate driven majorly by a master transcription factor (TF). Thus, a toggle switch between two TFs A and B often enable two mutually exclusive states: (high A, low B) and (low A, high B), corresponding to a specific phenotype.

The naïve CD4+ T-cells can differentiate into many Th phenotypes. Among these, the Th1, Th2 and Th17 phenotypes are each driven by a 'master regulator' TF (T-bet for Th1, GATA3 for Th2 and RORγT for Th17) that inhibits the other two. Thus, a network of three mutually repressing regulators (A, B and C) serves as a model for CD4+ T-cell differentiation (**Fig 1A**). We have previously shown that such a 'toggle triad' among A, B and C can enable three predominant states – (high A, low B, low C), (low A, high B, low C) and (low A, low B, high C) (represented by Abc, aBc and abC correspondingly hereafter) (Duddu *et al.*, 2020).

To characterize the dynamical repertoire enabled by a toggle triad, we mapped a phase diagram for the parameter sets enabling tristability corresponding to these three predominant states. We used the degradation rates of B and C (kB and kC) as the bifurcation parameters for this phase diagram (**Fig 1B**) to identify the influence of relative stability (or abundance) of A, B and C on different phenotypes. Starting from the tristable region enabling all three phenotypes (marked by R1: {Abc, aBc, abC}), as the degradation rate of B (kB) is increased, the state aBc (low A, high B, low C) ceases to exist and the system transitions into a bistable region with both states having antagonistic expression of A and C but low levels of B in both of them (marked by R2: {Abc, abC}). Similarly, after a threshold value of degradation rate of C (kC) is crossed, the state abC no longer exists and the system correspondingly transitions into a different bistable region (marked by R3: {Abc, aBc}). When both these degradation rates are increased simultaneously, the system can converge to only one state: (high A, low B, low C) (region R4: {Abc}). Similarly, from the regions R2 (R3), increasing the degradation rate of C (B), the

system can transition into region R4. Consistent trends were seen when we varied relative production rates instead of degradation rates (**Fig S1**).

Further, we performed stochastic simulation for these scenarios for representative parameter sets (values of kB and kC marked in **Fig 1B**) corresponding to regions R1-R4: R1 (kB = 1, kC = 0.5), R2 (kB = 2.5, kC = 1), R3 (kB = 1, kC = 1.5) and R4 (kB = 2.5, kC = 2). These simulations reveal switching among different possible phenotypes for corresponding regions from the phase diagram (**Fig 1C**). In the region R4, while stochastic fluctuations in levels of A are observed, these fluctuations do not impact levels of B and C (because both of them are at already very low levels due to increased degradation) and thus do not correspond to switching.

In the context of CD4 T-cell differentiation, R1 region indicates switching among Th1, Th2 and Th17; R2 and R3 correspond to switching among two possible phenotypes ({Th1, Th17}, {Th2, Th17} or {Th1, Th2}); R4 corresponds to an individual cell-state with no switching to another phenotype but with baseline heterogeneity due to biological noise (Th1, Th2 or Th17). Together, these results indicate that depending on the relative abundance of T-bet, GATA3 and RORγT, cells can exist in one or more of the three dominant phenotypes (Th1, Th2 and Th17) and can switch back and forth under the influence of stochastic fluctuations (biological noise). Such state-switching can induce and maintain phenotypic heterogeneity in a given T-helper cell population, with the relative frequencies of Th1, Th2 and Th17 dependent on relative levels of the master regulators (or equivalently, the concentration of different cytokines which can drive various cell-fates through their action on these master regulators).

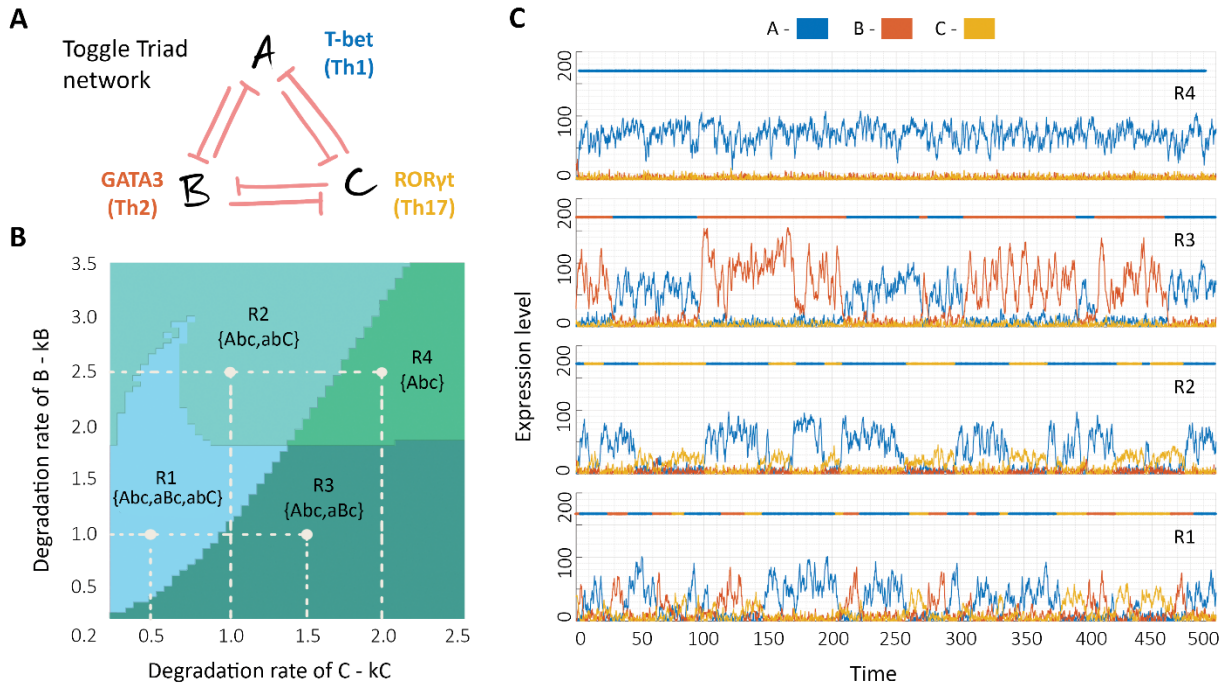


***Fig 1: Phenotypic heterogeneity in T-helper cell population. A)*** *Toggle Triad network topology underlies the differentiation of naïve CD4+ T-cell into T-helper cells (Th1, Th2 and Th17). Each master regulator (T-bet, GATA3 and RORγT respectively) mutually represses the other two.* ***B)*** *Phase diagram of network dynamics with bifurcation parameters as degradation rates of C (kC) and B (kB). Different regions (R1: tristability – {Abc, aBc, abC}; R2: bistability – {Abc, abC}, R3: bistability – {Abc, aBC}, R4: monostability –*

*{Abc}) are marked.* ***C)*** *Stochastic simulations of the network for various representative parameter sets (marked in B) with varying degradation rates of C and B (all other parameter values being the same) corresponding to each of the four marked regions in phase plot. Parameter values provided in Table S1. Bars drawn above represent corresponding phenotype – Abc (state A), aBc (state B) and abC (state C).*

**Epigenetic repression driven by a master regulator can enrich for its corresponding phenotype in a heterogeneous population**

Besides mutual repression at a transcriptional level, the three 'master regulators' (T-bet, GATA3 and RORγT) can engage in epigenetic mutual repression as well. To incorporate epigenetic repression in our framework, we utilized a phenomenological model approach (Miyamoto *et al.*, 2015) that introduces an epigenetic parameter (α) to quantify the threshold (half-maximal) levels corresponding to the influence of expression levels of one node on its target. The higher the value of α corresponding to a network edge, the stronger is the epigenetic repression incorporated in that interaction. The underlying idea behind this framework is that epigenetic repression serves as a self-stabilizing mechanism to capture that the longer a node stays at a high expression level, the more unlikely it is for the node to switch to a lower expression level (due to chromatin and/or DNA methylation changes it may have mediated meanwhile). Here, we use this framework to simulate multiple scenarios, i.e. epigenetic repression incorporated on various edges in a network, and quantify the changes in phenotypic distribution in a differentiating T-cell population (Th1, Th2, Th17), in presence of noise to account for stochastic effects.

First, we considered the scenario of epigenetic repression mediated by one of the master regulators (say, A) on inhibitory links to other two nodes (from A to B, and from A to C) (**Fig 2A**). The population distribution is calculated by considering multiple initial conditions (here, 1000), each representing an individual cell. The trajectory of each initial condition (cell) is followed, and the expression values of A, B and C are noted. Depending on the expression levels of the nodes, the state (of the cell) is defined and the population distribution is deduced. Noise is incorporated into the system at definite time intervals (See Methods). For a given tristable parameter set, we first identified population distribution in absence of any epigenetic repression ($\alpha_{AB} = 0$, $\alpha_{AC} = 0$) – approximately 25% cells were present in (high A, low B, low C) (Abc or state A) and in (low A, high B, low C) (aBc or state B) states, while 50% cells exhibited a (low A, low B, high C) (abC or state C) phenotype (**Fig 2B**, left bottom panel).

As we increase the strength of epigenetic repression from A to C ($\alpha_{AC}$), we observe a decrease in population the percentage of abC (or C) state and a corresponding increase in that corresponding to A and B. At ($\alpha_{AB} = 0$, $\alpha_{AC} = 0.2$), the system displays a population percentage distribution of about 33% A, 33% B and 33% C. This trend continues with further increase in value of $\alpha_{AC}$; at ($\alpha_{AB} = 0$, $\alpha_{AC} = 0.3$), a population distribution around 40% A, 30% B and 30% C is observed (**Fig 2B**, left column). Incorporating epigenetic repression from A to B ($\alpha_{AB}$) in addition to $\alpha_{AC} = 0.3$ further increases the population percentage corresponding to A. At ($\alpha_{AB} = 0.3$, $\alpha_{AC} = 0.3$), the population predominantly consists of cells in state A (75%) (**Fig 2B**, top row). This trend is further exemplified by the phase plot showing that the population percentage of A is minimum at low values of ($\alpha_{AB}$, $\alpha_{AC}$) and increases sharply as ($\alpha_{AB}$, $\alpha_{AC}$) values increase (**Fig 2B**).We performed similar analysis for other tristable parameter sets and observed similar trends, although the degree of enrichment of state A varied (**Fig 2C**). While the parameter set P1 shows a drastic increase in population percentage of A from 5% to 95%, P4 and P5 sets do not show huge shifts in phenotypic distributions – from 70% to 90% in P4 and from 85% to 95% in P5.

Put together, we conclude that including epigenetic repression from interactions originating from one of the three nodes in a toggle triad help increase the percentage of cells in a state for which that node serves as a 'master regulator'. The magnitude of change in phenotypic composition depends the strength of epigenetic feedback of either or both interactions. Extrapolating these results in the context of T-cell differentiation, they imply that if T-bet can mediate epigenetic repression on GATA3 and/or RORγT, the population predominantly will consist of Th1 cells. Similarly, Th2 (or Th17) cells can be the predominant phenotype in a heterogeneous T-cell population if GATA3 (or RORγT) can repress T-bet and RORγT (or T-bet and GATA3).

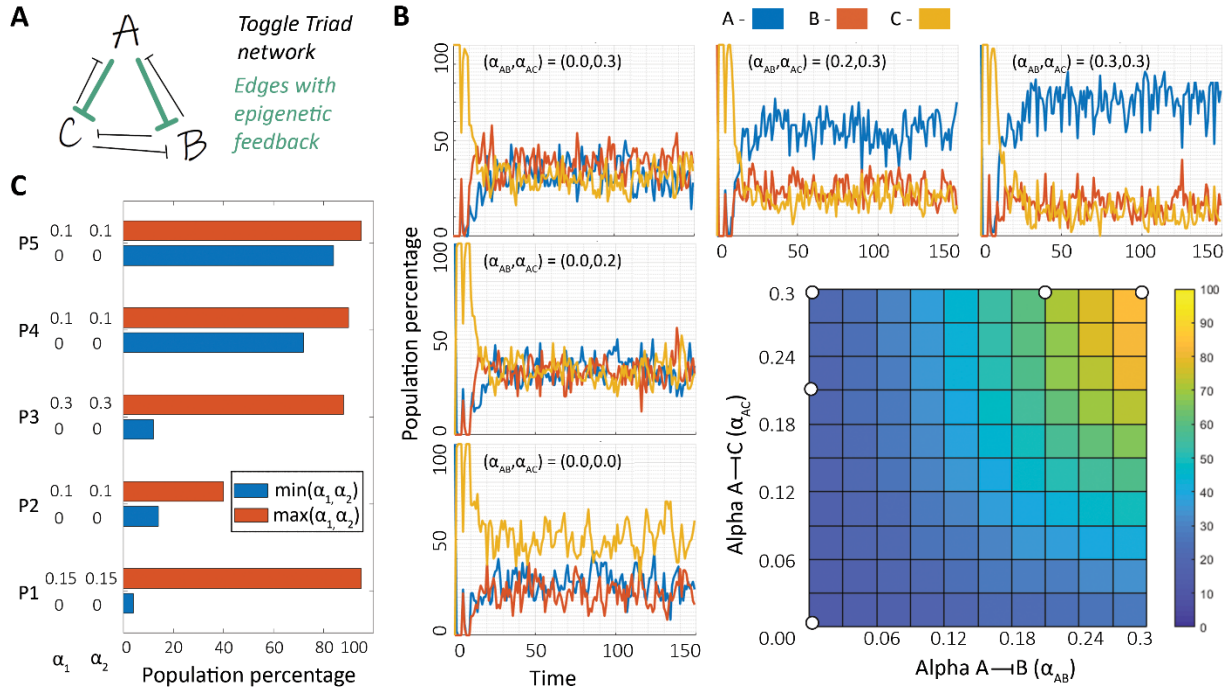


***Fig 2: Epigenetic repression mediated by one node in toggle triad on the other two nodes. A)*** *Toggle triad network topology in which interactions incorporating epigenetic repression are marked in green.* ***B)*** *Phase plot showing the population percentage of cells in state A (Abc) with bifurcation parameters as the α values corresponding to the epigenetic feedback of A-\|B and A-\|C, as well as dynamics of distribution of population percentage between states A, B and C for certain pairs of* $\alpha_{AB}$ *and* $\alpha_{AC}$ *values.* ***C)*** *Population percentage of the node from which interactions with epigenetic feedback originate with pair of α values at corresponding maximum and minimum for five different parameter sets. Parameter set P3 is used for simulations in* ***C.*** *Parameter values provided in Table S1.*

### Impact of competing and complementing epigenetic repression driven by two master regulators on the population distributions

Next, we consider the scenario of epigenetic repression incorporated on a pair of mutual repressive links (marked by green in **Fig 3A**: here, inhibition between A and B is considered). The strength of epigenetic repression is characterized by corresponding α values $\alpha_{AB}$ and $\alpha_{BA}$. For the given parameter set, the systems converges to approximately 45% A, 30% B and 25% C in absence of any epigenetic

repression ($\alpha_{AB} = 0$, $\alpha_{BA} = 0$) (**Fig 3A**). Increasing either $\alpha_{AB}$ or $\alpha_{BA}$ increases the population percentage corresponding to state A or B respectively: at ($\alpha_{AB} = 0.15$, $\alpha_{BA} = 0$), population distribution is about 70% A, 10% B and 20% C, while at ($\alpha_{AB} = 0$, $\alpha_{BA} = 0.15$), the heterogeneous population comprises of 25% A, 45% B and 30% C. Increasing both $\alpha_{AB}$ and $\alpha_{BA}$ values brings the population closer to the case of no epigenetic influence; at ($\alpha_{AB} = \alpha_{BA} = 0.15$), the population distribution comprises of approximately 50% A, 20% B and 30% C. Quantifying the ratio of population percentages corresponding to states A and B with $\alpha_{AB}$ and $\alpha_{BA}$ as the bifurcation parameters, we observed skewed ratios when one of the epigenetic repression links is much stronger than the other ( > 7 at $\alpha_{AB} = 0.15$, $\alpha_{BA} = 0$; and < 1 at $\alpha_{AB} = 0$, $\alpha_{BA} = 0.15$) (**Fig 3B**). Similar analysis for other parameter sets P2 and P3 (**Fig 3C**) substantiates these trends, where the ratio of population percentages of two representative states A and B is skewed when one of the links dominates (($\alpha_{1\text{-min}}$, $\alpha_{2\text{-max}}$) and ($\alpha_{1\text{-max}}$, $\alpha_{2\text{-min}}$)) but not when the epigenetic influence on one another is of comparable strengths (($\alpha_{1\text{-min}}$, $\alpha_{2\text{-min}}$) and ($\alpha_{1\text{-max}}$, $\alpha_{2\text{-max}}$)).

In the context of T-cell differentiation, these results imply that if T-bet and GATA3 can repress the expression or function of each other at an epigenetic level, the relative strength of their epigenetic inhibitions governs the relative proportions of Th1 and Th2 in a heterogeneous population. Similar statements can be made for mutual repression between any other pair of 'master regulators' here.

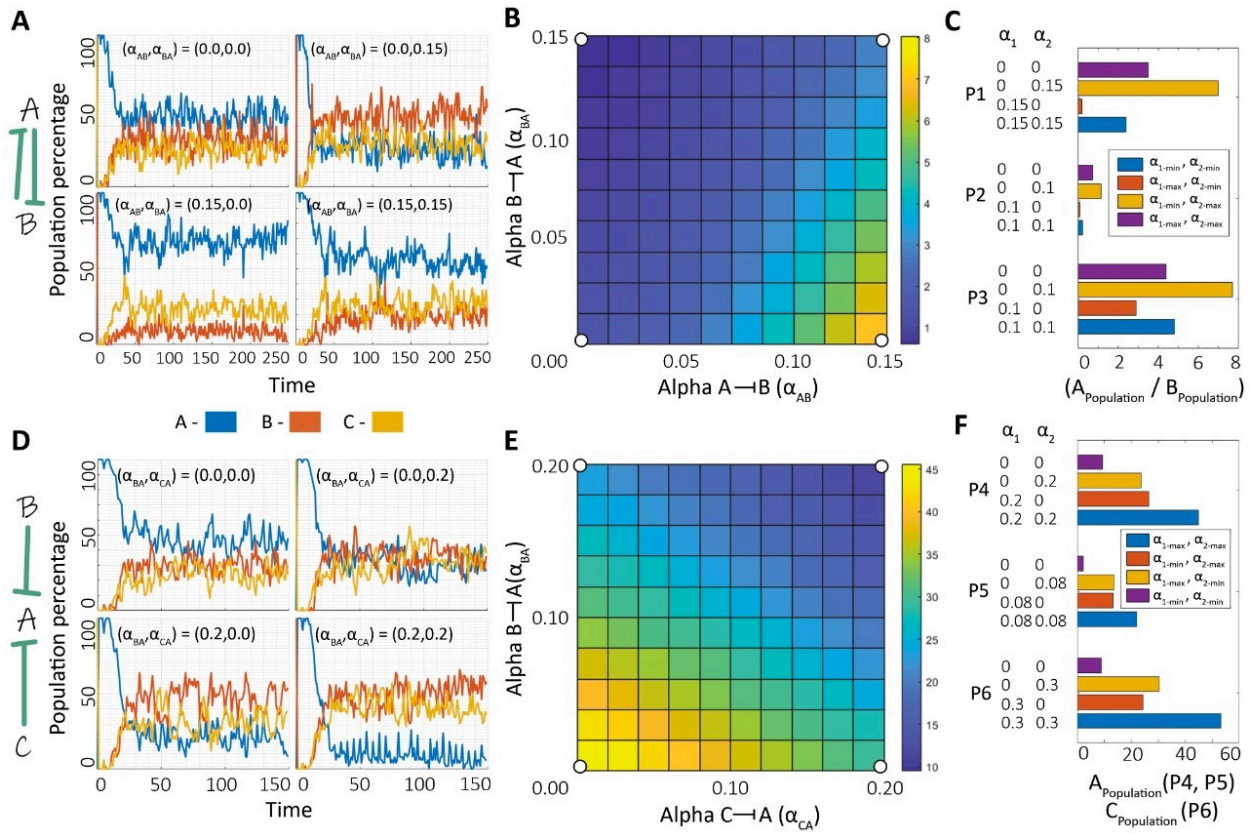


***Fig 3: Epigenetic repression on edges originating from more than one node in the toggle triad. A)*** *(Left) Toggle triad network in which interactions where epigenetic repression is incorporated are marked in green. (Right) Dynamics of distribution of population percentage between states A, B and C for certain pairs of $\alpha_{AB}$ and $\alpha_{BA}$ values.* ***B)*** *Phase plot showing the ratio of population percentage of A to that of B with*

*bifurcation parameters as the α values corresponding to the epigenetic feedback of A-|B and B-|A.* ***C)*** *Ratio of population percentages of the nodes from which interactions with epigenetic feedback originate with pair of α values at combinations of maximum and minimum for three different parameter sets.* ***D)*** *(left) same as A). (right) same as A) but for certain pairs of $\alpha_{CA}$ and $\alpha_{BA}$ values.* ***E)*** *Phase plot showing the population percentage of A with bifurcation parameters as the α values corresponding to epigenetic feedback of C-|A and B-|A.* ***F)*** *Population percentage of A (for parameter set P4 and P5), that of C (for parameter set P6) for given α values ($\alpha_{CA}$ and $\alpha_{BA}$ in P4, P5; $\alpha_{AC}$ and $\alpha_{BC}$ in P6). Parameter sets P1 and P4 are used for simulations in* ***B*** *and* ***E*** *respectively. Parameter values provided in Table S1.*

Finally, we considered a scenario where both epigenetic repression is incorporated on two edges terminating at a single node of the toggle triad (marked in green in **Fig 3D**; here, inhibition of A by B and by C). The strength of the epigenetic feedback is characterized by corresponding α values, $\alpha_{BA}$ and $\alpha_{CA}$ respectively. Without any epigenetic feedback ($\alpha_{BA} = 0$, $\alpha_{CA} = 0$), the system equilibrates to a population percentage distribution of 45% A, 30% B and 25% C (**Fig 3D**). Increasing either $\alpha_{BA}$ or $\alpha_{CA}$ decreases the population percentage corresponding to state A (Abc); at both ($\alpha_{BA} = 0.2$, $\alpha_{CA} = 0$) and ($\alpha_{BA} = 0$, $\alpha_{CA} = 0.2$), the population percentage corresponding to state A drops to 20 – 25%. Increasing both $\alpha_{BA}$ and $\alpha_{CA\ further}$ reduces the population percentage of state A (10% A at ($\alpha_{BA} = 0.2$, $\alpha_{CA} = 0.2$)) (**Fig 3D, E**). Similar trends are seen for other parameter sets P5 and P6, where epigenetic repression on both the incoming edges to a node seem to act independently and additively (**Fig 3F**). Results for other parameter sets and representative scenarios (B inhibiting A and C epigenetically; B and C epigenetically inhibit each other; B and C inhibiting A epigenetically) show consistent trends as abovementioned (**Fig S2-S4**).

Together, these three different scenarios underscore how epigenetic repression incorporated through different inhibitory edges in T-bet/GATA3/RORγT regulatory network can alter the population distribution structure (% of Th1, Th2, Th17) in a T-cell differentiation context.

**The impact of epigenetic influence on population distribution depends both on corresponding strength(s) and duration(s)**

So far, we have considered epigenetic feedback on any edge to be either constantly present or absent. Next, we characterize the dynamics of the system with the epigenetic feedback provided only for certain time duration instead of being present constantly (throughout the simulation) as previously.

First, we choose a bistable parameter set (here {aBc, abC}), as shown in stochastic simulations (**Fig 4A**). Epigenetic feedback is provided to inhibition of B by C (**Fig 4B**). We then performed dynamic simulation of the system to obtain expression levels of the three nodes A, B and C with and without epigenetic feedback and for a given initial condition (cell). We see a switch in the state from {aBc} to {abC} when epigenetic repression is included; the levels of A are maintained low as expected (**Fig 4C**). At the population level, no cell exhibits state A, consistent with the bistable nature of the system. In absence of epigenetic influence, the states B and C constitute 70% and 30% of the steady-state population distribution. In presence of epigenetic influence, this distribution changes to 40% and 60% respectively at $\alpha_{CB} = 0.3$, and 30% and 70% respectively as the strength of repression is further increased ($\alpha_{CB} = 0.5$) (**Fig 4D**). For both these values of $\alpha_{CB}$, the magnitude of change in population distribution increases with the value of X (the time for which epigenetic influence was included), indicating that both the dose and duration of epigenetic repression can alter population distribution.

Next, we considered a tristable parameter set where epigenetic repression was incorporated on two interactions terminating on the same node (**Fig 4E**; A and C both inhibiting B; strengths: $\alpha_{AC}$ and $\alpha_{BC}$). We switched on the epigenetic feedback for only a certain fraction of the entire simulation time (X: here, 50 arbitrary units). Without any epigenetic feedback, the population converged to 15% cells in state A, 15% in state B and 70% in state C (**Fig 4F**). As X is increased, the population percentage corresponding to state C decreases while that corresponding to states A and B concomitantly increase. Finally, we varied both the parameters – X and $\alpha_{AC}$ (= $\alpha_{BC}$) – to draw a phase plot. The population percentage corresponding to state C is about 70% at $\alpha_{BC} = \alpha_{AC} = 0$ and a short duration ($\log_{10}X = -3$). At low strength ($\alpha_{BC} = \alpha_{AC} < 0.1$) and short durations ( $-3 < \log_{10}X < -2$) corresponding to epigenetic repression, no major changes are observed for the population distribution (left bottom part in **Fig 4G**). However, beyond this approximate threshold (marked by an asterisk in **Fig 4G**), increasing either the strength or the duration (vertical and horizontal arrows in **Fig 4G**) leads to comparable and pronounced decreased in the population corresponding to state C. Put together, we conclude that both the factors – strength of epigenetic silencing (α) or the time duration for which it is switched on (X) – can act independently and alter the population distribution patterns, given a threshold amount of the other. These two variables seem to have additive and complementary effects rather than redundant ones.

In terms of T-cell differentiation, these results indicate that either a strong epigenetic silencing of other cell lineages for a short duration or a gradually accumulating impact of epigenetic silencing can both drive changes in population heterogeneity, suggesting an 'area under the curve' dynamical principle.

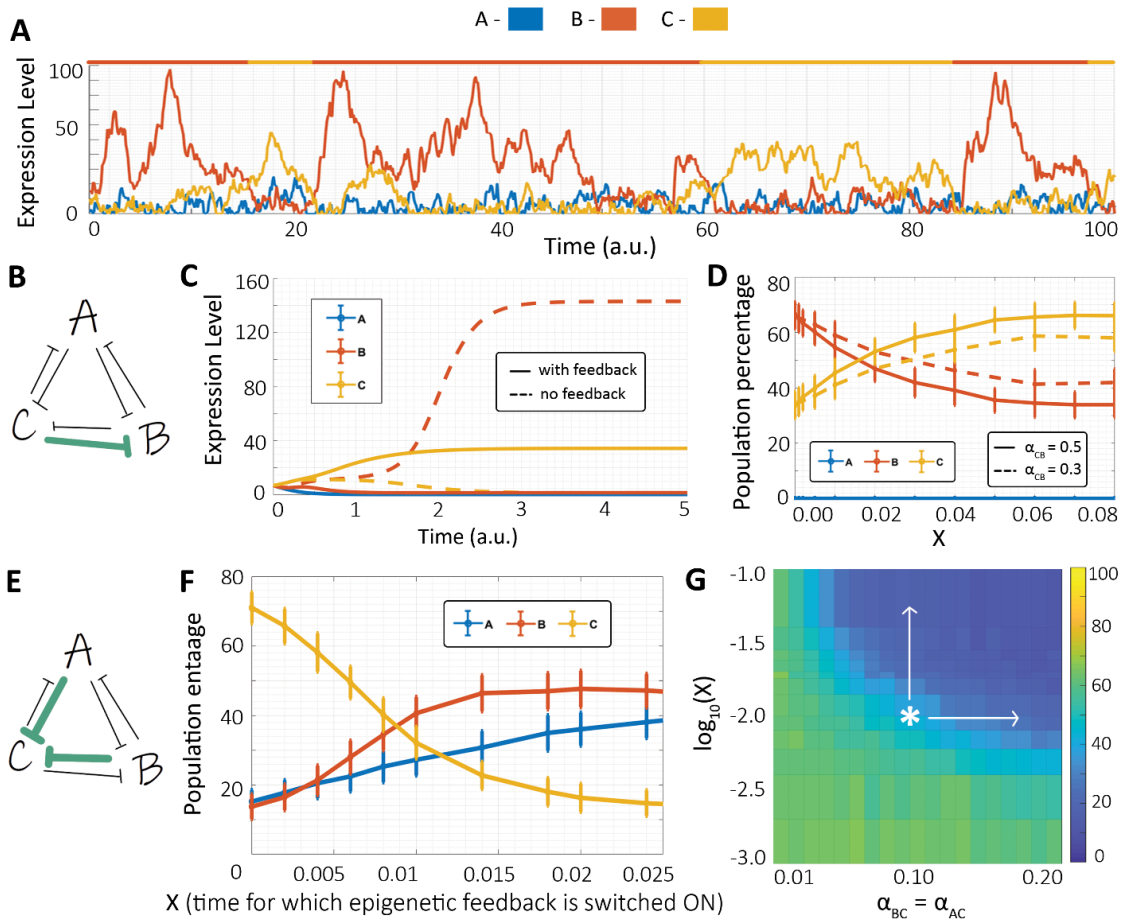

***Fig 4: Epigenetic repression on edges originating from more than one node in the toggle triad. A)*** *Stochastic simulation of the Toggle Triad network with a parameter set enabling bistability with the state {aBc, abC}.* ***B)*** *Toggle Triad network topology in which interactions marked in green are being provided with epigenetic feedback for the same parameter set used in D.* ***C)*** *Dynamics simulation of the network with same initial condition but with and without epigenetic feedback to the marked interaction.* ***D)*** *Population percentages of A, B and C as X, the fraction of time (here over 50 time arbitrary units) for which the epigenetic feedback for marked interaction is switched ON and then turned OFF, for two values of the feedback strength given by* $\alpha_{CB}$. ***E)*** *Toggle Triad network topology in which interactions marked in green are being provided with epigenetic feedback* ***F)*** *Population percentages of A, B and C as X, the fraction of time (here 50 time arbitrary units) for which the epigenetic feedback for both marked interactions is switched ON and then turned OFF.* ***G)*** *Phase plot showing population percentage of C (node on which interactions with epigenetic feedback terminate) with bifurcation parameters as the α value corresponding to the epigenetic feedback of A-|C and B-|C (both same so considered on single axis) and* $\log_{10}(X)$*, a metric of X. Parameter values provided in Table S1.*

Previously, we considered varying values of $\alpha_{AC} = \alpha_{BC}$ and observed how this feedback strength and X affect the phenotypic heterogeneity of the population distribution. Next, we consider a more generic scenario where $\alpha_{AC}$ and $\alpha_{BC}$ values need not be identical. Also, instead of including the epigenetic influence on only incoming links on C (C being inhibited by A and B), we now also incorporate the epigenetic influence of C inhibiting A and/or B, to represent the mutual epigenetic repression scenario.

First, we choose a tristable parameter set ({Abc, aBc, abC}) and include epigenetic influence from C to B with ($\alpha_{CB} = 0.2$). We can continuously decrease the strength of this influence, i.e. $\alpha_{CB}$ varies between 0 and 0.2, and increase the epigenetic influence from B on C ($\alpha_{BC}$). Thus, similar to mutual repression as seen at a transcriptional level in a toggle switch (Gardner *et al.*, 2000), two nodes can also inhibit each other at an epigenetic level as well. The difference between the two parameters ($\alpha_{BC} - \alpha_{CB}$) indicates which epigenetic repression (from B to C or from C to B) is predominant. Thus, we varied two parameters – $\alpha_{BC} - \alpha_{CB}$ and X – and obtained the phase plots corresponding to percentage population in the three states: Abc (state A), aBc (state B) and abC (state C) (**Fig 5A, i-iii** respectively). As $\alpha_{BC} - \alpha_{CB}$ changes from -0.2 to 0.2, i.e. as the epigenetic influence of B inhibiting C takes over that of C inhibiting B, and given a minimal critical value of X (= 0.01), the population corresponding to state B increases from about 12% to about 20%. For the same change in parameters, population for state C decreases correspondingly from about 78% to about 70%. But, for the same change in epigenetic influence at a higher value of X (= 0.03), the change in population corresponding to state B is more drastic (from 12% to 40%), with a correspondingly sharp fall in population corresponding to state C (from 80% to 50%). Similar trends are noted for a different representative example of mutual epigenetic repression is considered (i.e. when A and C inhibit each epigenetically) (**Fig S5A**).

Next, we investigate the scenario of mutual epigenetic repression for two toggle switches instead of just one: between B and C, as well as between A and C. Thus, in addition to changes in $\alpha_{BC} - \alpha_{CB}$, $\alpha_{AC} - \alpha_{CA}$ can also be considered as a parameter to be varied. For this parameter set, while $\alpha_{BC} - \alpha_{CB}$ changes from -0.2 to 0.2, $\alpha_{AC} - \alpha_{CA}$ changes from -0.05 to 0.15. We observed that at X= 0.03, as the magnitude of the incoming epigenetic repression on C increases as compared to the ability of C to epigenetically repress A and/or B (i.e., $\alpha_{BC} - \alpha_{CB} > 0$ and $\alpha_{AC} - \alpha_{CA} > 0$), the population corresponding to state C drops sharply from 80% to 15%, with corresponding increase in population corresponding to both the states A and B (from 10% to 35% for A, and from 10% to 45% for B) (**Fig 5B, i-iii**).

Finally, we consider the case of a fixed duration for which epigenetic repression is switched ON (X = 0.03), but vary the difference in the strengths of epigenetic repression between two 'master regulators' to draw the phase plot of population corresponding to the three states (**Fig 5C**). We noticed that for this parameter set, the population corresponding to state A changes more along the x-axis ($\alpha_{AC}$ - $\alpha_{CA}$) than along the y-axis ($\alpha_{BC}$ - $\alpha_{CB}$), i.e. the frequency of state A is more sensitive to changes in mutual epigenetic repression between A and C than those between B and C (**Fig 5C, i**). Similar trend is observed is seen for node B initially (i.e. change in the frequency of state B is more prominent along the y-axis ($\alpha_{BC}$ - $\alpha_{CB}$) than along the x-axis ($\alpha_{AC}$ - $\alpha_{CA}$)), but at higher values of $\alpha_{AC}$ - $\alpha_{CA}$, the population corresponding to state B is also affected (**Fig 5C, ii**). Because C is involved in both the instances of mutual epigenetic repression (i.e., with B and with A), the population corresponding to state C falls with an increase in incoming epigenetic repression from either node – A or B. When C is maximally repressing A and B at an epigenetic level (left bottom part of **Fig 5C, iii**), the population corresponding to state C is 80%. At the values corresponding to (maximum $\alpha_{AC}$, minimum $\alpha_{BC}$) and (minimum $\alpha_{AC}$, maximum $\alpha_{BC}$) (top left and right bottom parts of **Fig 5C,iii**), the population corresponding to state C falls to 60% and 55% respectively. At the value corresponding to (maximum $\alpha_{AC}$, maximum $\alpha_{BC}$), the population of C decreases to 15% (top right part of **Fig 5C,iii**). Besides depending on the difference in corresponding α values, changes in population distribution can depend on X too (**Fig S5B-C**).

In terms of T-cell differentiation, these results imply that if the extent of epigenetic repression on one of the three 'master regulators' is strong enough as compared to the repression it can mediate on one or both of other two 'master regulators', the corresponding phenotypic frequency will decrease majorly.

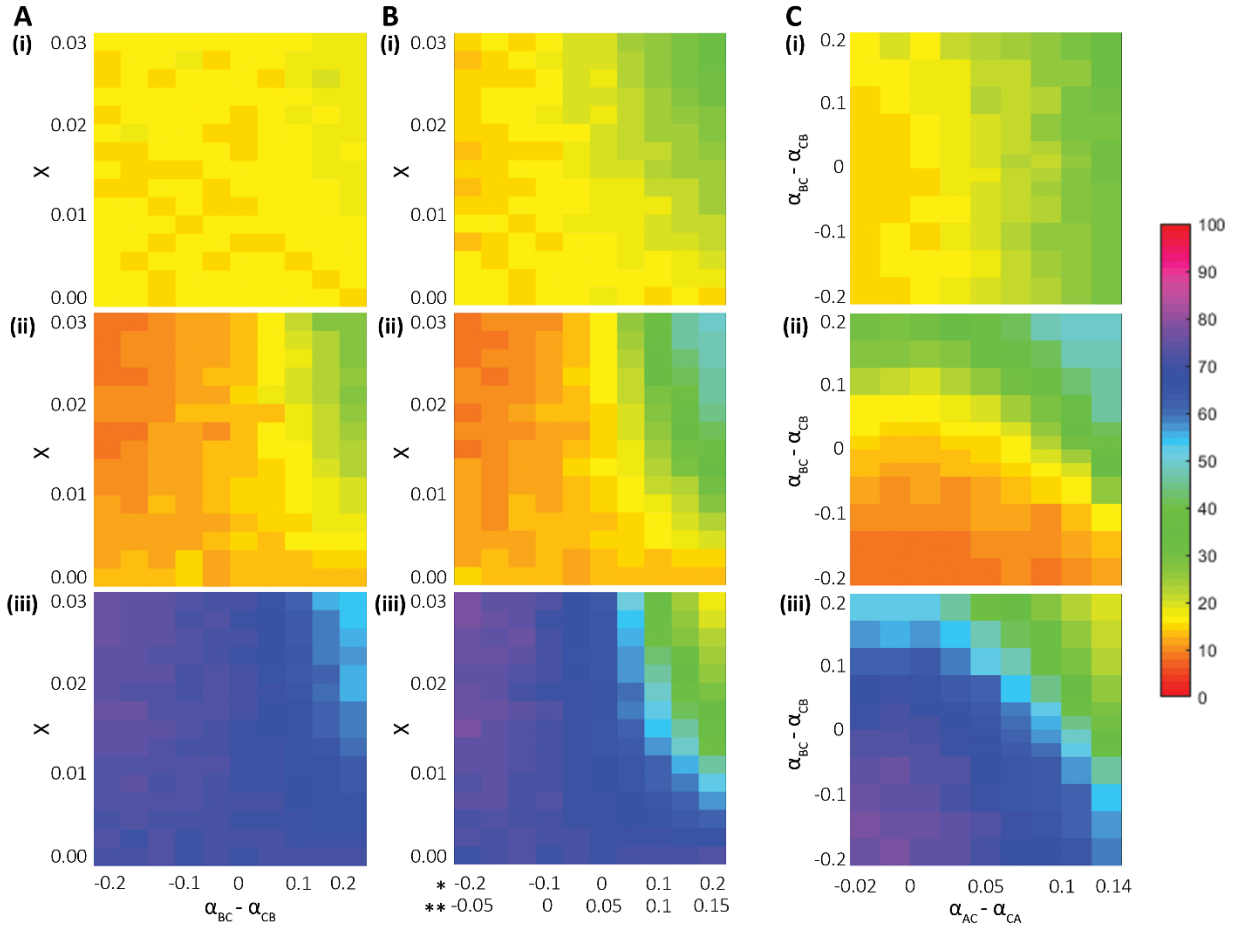

***Fig 5: Varying the epigenetic repression from a node to onto the node in toggle triad. A) i)*** *Phase plot of population percentage corresponding to node A with variations in two parameters: X and the relative epigenetic influence which is varied from a case of stronger repression from C to B ($\alpha_{BC} < \alpha_{CB}$) to a stronger repression from B to C ($\alpha_{BC} > \alpha_{CB}$)* ***ii)*** *Same as i) but for state B.* ***iii)*** *Same as i) but for state C.* ***B) i)*** *Same as A; i) but for varying relative epigenetic influence in both feedback loops (between A and C, and between B and C). Corresponding $\alpha_{BC} - \alpha_{CB}$ and $\alpha_{AC} - \alpha_{CA}$ values are given on x-axis, marked by * and ** respectively.* ***ii)*** *Same as i) but for state B.* ***iii)*** *Same as i) but for state C.* ***C) i)*** *Phase plot of population percentage corresponding to state A with bifurcation parameters as the difference in α values corresponding to mutual epigenetic repression ($\alpha_{BC} - \alpha_{CB}$ and $\alpha_{AC} - \alpha_{CA}$), at X = 0.03.* ***ii)*** *Same as i) but for state B.* ***iii)*** *Same as i) but for state C. Parameter values provided in SI table 1.*

## Discussion

Gaining a predictive understanding of the dynamics of cell-fate decisions is instrumental for decoding cell differentiation during development and homeostasis, and modulating it in pathological scenarios. Cell-fate decisions, including those seen in naïve helper T-cell differentiation into Th1, Th2 and Th17 cells, are the emergent outcomes of an entangled interplay of various levels of regulatory control – transcriptional (Evans and Jenner, 2013; Pillai and Jolly, 2021), translational (Liu *et al.*, 2018; Sarkar *et al.*, 2019), alternative splicing (Jolly *et al.*, 2018; Radens *et al.*, 2021), epigenetic (Wilson *et al.*, 2009; Jia *et al.*, 2019) and metabolic (Stark *et al.*, 2019; Jia *et al.*, 2021) among others. Recent efforts have begun to identify the dynamics of cell-fate decisions by investigating time-course transcriptional data (Pedicini *et al.*, 2010; Intosalmi *et al.*, 2015; Cook and Vanderhyden, 2020; Deshmukh *et al.*, 2021). However, how the different regulatory layers operating at varying time scales orchestrate coordinated cell decision-making at an individual cell and cell population level remains largely unclear.

Here, we investigate the dynamics of coupled transcriptional-epigenetic regulation in a network of three mutually repressing nodes forming a toggle triad. Analyzing the dynamics of a toggle triad can help elucidate CD4+ helper T-cell differentiation into Th1, Th2 and Th17 cells, given that each of the master regulator (T-bet, GATA3 and RORγT) can repress the other two at transcriptional and/or epigenetic levels directly or indirectly. We incorporated a simple phenomenological model to include epigenetic influence (Miyamoto *et al.*, 2015) to demonstrate how varying strengths of epigenetic repression can alter the stability of the three cell states (Th1, Th2 and Th17) and consequently alter the proportion of these phenotypes in a differentiating CD4+ T-cell population. The stronger the epigenetic repression mediated by a master regulator, the higher the predominance of corresponding phenotype in a cell population.

Our model predicts that besides its strength, the duration for which epigenetic repression is 'active' can modulate the population heterogeneity during helper T cell differentiation. Specifically, a weaker epigenetic repression for longer times and a stronger repression for shorter times has similar outcomes; this prediction can help plan next experiments to decode T-cell differentiation as a function of varying cytokine doses and durations. Thus, unlike previous mathematical models for CD4+ T-cell differentiation mostly focused on steady-state analysis at a transcriptional level (Hong *et al.*, 2011; Martinez-Sanchez *et al.*, 2018; Puniya *et al.*, 2018), our model incorporates the epigenetic-driven dynamics of plasticity and heterogeneity among the Th1, Th2 and Th17 phenotypes in a CD4+ T-cell population.

Phenotypic heterogeneity has been reported *in silico* (Martinez-Sanchez *et al.*, 2018; Puniya *et al.*, 2018), *in vitro* and *in vivo* in the presence of a mixture of cytokines driving different T-cell phenotypes (Han *et al.*, 2014; Becattini *et al.*, 2015; DuPage and Bluestone, 2016; Eizenberg-Magar *et al.*, 2017; DiToro and Basu, 2021; van Beek *et al.*, 2021). Our model predicts that multistability in T-bet/GATA3/ RORγT regulatory network can allow for phenotypic switching and heterogeneity as its inherent dynamical property, similar to other regulatory networks driving 'sibling' cell fates (Zhou and Huang, 2011). Another dynamical feature of multistable systems is the presence of both stability (for individual phenotypes) and plasticity (among many phenotypes), and epigenetic remodeling may alter the balance between them. For instance, differences in chromatin marks may alter the propensity of an epithelial cell to switch to a mesenchymal phenotype under the influence of an inducer (Eichelberger *et al.*, 2020; Jia *et al.*, 2020). Similarly, a subset of Th2 cells have been shown to not express T-bet and IFNγ when stimulated under Th1 conditions (Messi *et al.*, 2003). Recent "cross-polarization" experiments highlighted such "limited but detectable functional plasticity" for a population of Th1, Th2 and Th17 cells, indicating that these phenotypes represent relatively stable entities (Tortola *et al.*, 2020). Epigenetic marks are considered to help maintain such stability and heritability of cell-fate decisions (Wilson *et al.*, 2009), but whether epigenetic differences underlie such heterogeneity in response (stability vs. plasticity) in a cell population needs further investigation (van Beek *et al.*, 2021). Preliminary evidence in Th1 cells pinpoints that permissive chromatin modifications coincide with the ability of Th1 cells to express IL-17 under Th17-polarizing conditions (Curtis *et al.*, 2010), but it falls short of establishing a causative connection. Our model simulations imply that epigenetic repression driven by master regulators can influence the rate of switching from one phenotype to another, thus offering a quantitative dynamic platform to measure the stability (heritability) vs. plasticity propensities.

The balance between plasticity and stability is likely to depend on phenotype-specific global mapping of chromatin marks such as H3K4me3 and H3K27me3 that associate with activation and repression of gene expression respectively (Wei *et al.*, 2009). Higher plasticity has been shown to be concurrent with the presence of bivalent chromatin (i.e. simultaneous presence of active and repressive marks) (Chaffer *et al.*, 2013). For instance, the *Foxp3* promoter is not epigenetically repressed in Th17 cells, possibly enabling Th17-Treg plasticity (Wei *et al.*, 2009). In our phenomenological model which does not explicitly capture the molecular details of epigenetic repression (Zhao *et al.*, 2021), a bivalent chromatin state can be conceptually mapped on to the regions of relatively weak epigenetic influence of one master regulator on others. Thus, the weaker the epigenetic influence of node A on node B ($\alpha_{AB}$) relative to that of node B on node A ($\alpha_{BA}$), the higher the expected plasticity of the phenotype driven by node A. Indeed, this trend is observed in our simulations both in terms of plasticity of phenotype and the consequent population distribution. Therefore, our model can possibly explain the high plasticity observed for Th17 cells observed in many contexts such as cancer and autoimmunity (Stadhouders *et al.*, 2018; Cerboni *et al.*, 2021). In other words, we propose that increased plasticity of Th17 cells may be a consequence of a) weak epigenetic repression driven by RORγT on T-bet and/or GATA3, and/or b) strong epigenetic repression mediated by T-bet and/or GATA3 on RORγT.

Together, despite the limitations of investigating a minimalistic regulatory network and incorporating epigenetic influence only at a phenomenological level, our model simulations offer valuable insights into the dynamics of phenotypic plasticity and heterogeneity in a CD4+ T-cell population comprising Th1, Th2 and Th17 phenotypes. We provide a platform to quantify the plasticity and stability of different phenotypes and the overall phenotypic distribution as a function of varying strengths of epigenetic influence mediated by the master regulators (T-bet, GATA3, RORγT) on one another in a toggle triad, leading to 'mexican standoff-like' situation among these nodes to govern phenotypic plasticity (**Fig 6**).

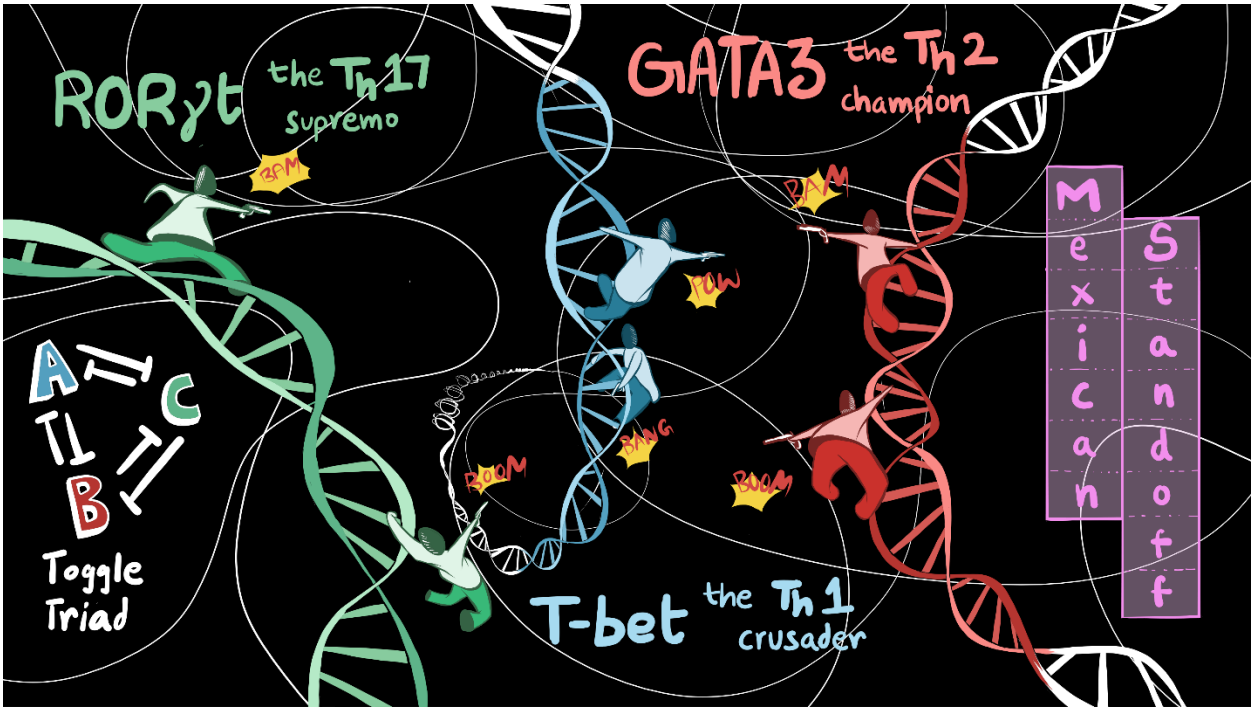


***Fig 6: A Mexican standoff schematic representing the CD4+ T-cell differentiation.***

**Author contributors** MKJ conceived and supervised research; ASD performed research; all authors contributed to data analysis and interpretation, and in preparing the manuscript.

**Acknowledgements** We thank Mr. Navin Vincent (IISc Bangalore) for help with the phase diagrams in Fig 1, S1.

**Conflict of Interest** The authors declare no conflict of interest.

**Funding** MKJ was supported by Ramanujan Fellowship (SB/S2/RJN-049/2018) awarded by Science and Engineering Research Board (SERB), Department of Science and Technology (DST), Govt. of India, and by InfoSys Young Investigator Fellowship awarded by Infosys Foundation, Bangalore. ASD acknowledges support by Prime Ministers' Research Fellowship (PMRF) awarded by Govt. of India.

**Data availability** All parameter sets used here are given in Table S1. All codes used are given at the following GitHub repository: https://github.com/csbBSSE/Toggle-Triad-Epigenetics

## Materials and Methods

### *RACIPE (RAndom CIrcuit PErturbation analysis)*

RACIPE is a computational tool that investigates the emergent dynamics of a given network topology [22]. A topology file is given as the input to the program. It then simulates, for every randomly chosen parameter set, the network as a system of ODEs developed based on the input file. For every run of the simulation, every kinetic parameter in mathematical model is sampled from the defined biologically relevant range, thus giving multiple parameter sets. RACIPE reports the steady-state values for each component of the network for every parameter set in the solution file. For all our analyses, we have used the default ranges for sampling the parameters, sampled 10 000 parameter sets and 1000 initial conditions for every parameter set. Depending on the number of steady states the system converges to for a given parameter set, the system is classified as monostable, bistable, tristable all the way to decastable. Even if one initial condition converges to a different steady state, RACIPE considers the system to be multi-stable for that parameter set. A generic differential equation for node A affected by node B is denoted by RACIPE as follows:

$$\frac{dA}{dt} = g_A \ * H^s(B, B^0A, nBA, \lambda BA) - k_A \ * A$$

where gA and kA are corresponding production and degradation rates, HS (B, B0A, nBA, λBA) denotes a shifted Hill function [22] defined as follows:

$$H^s(B, B^0A, nBA, \lambda BA) = H^-(B) + \lambda BA^*\big(1 - H^-(B)\big) \quad where, \ H^-(B) = \frac{1}{1 + \left(\frac{B}{B^0A}\right)^{nBA}}$$

From the final output provided by RACIPE, we chose certain parameter sets enabling tristability and bistability to conduct simulations.

### *Mathematical framework for epigenetic feedback*

The framework involves an iterative form of the equations used in RACIPE. The iterative form of equation for expression level of A, along with how noise is added into the system is given as follows:

$$A(i+1) = A(i) + \tau * [g_A * H(B, B^0A, nBA, \lambda BA) * H(C, C^0A, nCA, \lambda CA) - k_{A^*}A] + rand^* N$$

where, $A(i)$ is the expression level of node A at i$^{th}$ iteration, $\tau$ is the time step taken after every iteration, $rand$ is the random number generated in MATLAB and $N$ a magnitude factor to multiply noise with.

Noise is added at set intervals and not at every iteration. The threshold value of interaction at which epigenetic influence is added depends on strength of epigenetic feedback (α) as well as the expression level of the node from which the interaction originates. If epigenetic feedback is provided to the interaction A-|B, the iterative equation to continuously update the threshold would be as follows:

$$A^0B(i+1) = A^0B(i) + \tau * [\, a^0b - A^0B(i) - \big(\alpha_{AB} * A(i)\big)] * \frac{1}{\beta}$$

where, $A^0B(i)$ is threshold value of the inhibition from A to B at the i$^{th}$ iteration, $a^0b$ is the original value of threshold from the chosen parameter set, $\alpha_{AB}$ is a parameter modulating the strength of the epigenetic feedback along with $A(i)$ and $\beta$ is a scaling factor to control the rate of change of threshold value.

### *sRACIPE*

We used the webserver facility of Gene Circuit Explorer (GeneEx) to simulate stochastic dynamics of gene regulatory circuits: https://geneex.jax.org/.

## References


Becattini, S et al. (2015). T cell immunity. Functional heterogeneity of human memory CD4$^{+}$ T cell clones primed by pathogens or vaccines. Science 347, 400–406.

van Beek, JJP, Rescigno, M, and Lugli, E (2021). A fresh look at the T helper subset dogma. Nat Immunol 22, 104–105.

Cerboni, S, Gerhmann, U, Preite, S, and Mitra, S (2021). Cytokine-regulated Th17 plasticity in human health and diseases. Immunology 163, 3–18.

Chaffer, CL, Marjanovic, ND, Lee, T, Bell, G, Kleer, CG, Reinhardt, F, D'Alessio, AC, Young, RA, and Weinberg, RA (2013). Poised chromatin at the ZEB1 promoter enables breast cancer cell plasticity and enhances tumorigenicity. Cell 154, 61–74.

Chang, S, and Aune, M (2007). Dynamic changes in histone-methylation "marks" across the locus encoding interferon-gamma during the differentiation of T helper type 2 cells. Nat Immunol 8, 723–731.

Chatterjee, S et al. (2018). CD38-NAD + Axis Regulates Immunotherapeutic Anti-Tumor T Cell Response. Cell Metab 27, 85-100.e8.

Cherry, JL, and Adler, FR (2000). How to make a biological switch. J Theor Biol 203, 117–133.

Cook, DP, and Vanderhyden, BC (2020). Context specificity of the EMT transcriptional response. Nat Commun 11, 2142.

Curtis, MM, Rowell, E, Shafiani, S, Negash, A, Urdahl, KB, Wilson, CB, and Way, SS (2010). Fidelity of pathogen-specific CD4+ T cells to the Th1 lineage is controlled by exogenous cytokines, interferon-γ expression, and pathogen lifestyle. Cell Host Microbe 8, 163–173.

Deshmukh, AP et al. (2021). Identification of EMT signaling cross-talk and gene regulatory networks by single-cell RNA sequencing. Proc Natl Acad Sci U S A 118, e2102050118.

DiToro, D, and Basu, R (2021). Emerging Complexity in CD4+T Lineage Programming and Its Implications in Colorectal Cancer. Front Immunol 12, 694833.

Duddu, AS, Sahoo, S, Hati, S, Jhunjhunwala, S, and Jolly, MK (2020). Multi-stability in cellular differentiation enabled by a network of three mutually repressing master regulators. J R Soc Interface 17, 20200631.

DuPage, M, and Bluestone, JA (2016). Harnessing the plasticity of CD4+ T cells to treat immune-mediated disease. Nat Rev Immunol 16.

Eichelberger, L et al. (2020). Maintenance of epithelial traits and resistance to mesenchymal reprogramming promote proliferation in metastatic breast cancer. BioRxiv, 998823.

Eizenberg-Magar, I, Rimer, J, Zaretsky, I, Lara-Astiaso, D, Reich-Zeliger, S, and Friedman, N (2017). Diverse continuum of CD4+ T-cell states is determined by hierarchical additive integration of cytokine signals. Proc Natl Acad Sci U S A 114, E6647–E6456.

Evans, CM, and Jenner, RG (2013). Transcription factor interplay in T helper cell differentiation. Brief Funct Genomics 12, 499–511.

Fang, D, and Zhu, J (2017). Dynamic balance between master transcription factors determines the fates and functions of CD4 T cell and innate lymphoid cell subsets. J Exp Med 214, 1861–1876.

Gardner, TS, Cantor, CR, and Collins, JJ (2000). Construction of a genetic toggle switch in Escherichia coli. Nature 403, 339–342.

Graham, TGW, Tabei, SMA, Dinner, AR, and Rebay, I (2010). Modeling bistable cell-fate choices in the Drosophila eye: Qualitative and quantitative perspectives. Development 137, 2265–2278.

Han, A, Glanville, J, Hansmann, L, and Davis, MM (2014). Linking T-cell receptor sequence to functional phenotype at the single-cell level. Nat Biotechnol 32, 684–692.

Hari, K, Sabuwala, B, Subramani, BV, La Porta, CAM, Zapperi, S, Font-Clos, F, and Jolly, MK (2020). Identifying inhibitors of epithelial-mesenchymal plasticity using a network topology based approach. Npj Syst Biol Appl 6, 15.

Hirahara, K, Vahedi, G, Ghoreschi, K, Yang, XP, Nakayamada, S, Kanno, Y, O'Shea, JJ, and Laurence, A (2011). Helper T-cell differentiation and plasticity: Insights from epigenetics. Immunology 134, 235–245.

Hong, T, Xing, J, Li, L, and Tyson, JJ (2011). A Mathematical Model for the Reciprocal Differentiation of T Helper 17 Cells and Induced Regulatory T Cells. PLoS Comput Biol 7, e1002122.

Intosalmi, J, Ahlfors, H, Rautio, S, Mannerstöm, H, Chen, ZJ, Lahesmaa, R, Stockinger, B, and Lähdesmäki, H (2015). Analyzing Th17 cell differentiation dynamics using a novel integrative modeling framework for time-course RNA sequencing data. BMC Syst Biol 9, 81.

Jia, D et al. (2021). Towards decoding the coupled decision-making of metabolism and epithelial-to-mesenchymal transition in cancer. Br J Cancer 124, 1902–1911.

Jia, W, Deshmukh, A, Mani, SA, Jolly, MK, and Levine, H (2019). A possible role for epigenetic feedback regulation in the dynamics of the Epithelial-Mesenchymal Transition (EMT). Phys Biol 16, 066004.

Jia, W, Tripathi, S, Chakraborty, P, Chedere, A, Rangarajan, A, Levine, H, and Jolly, MK (2020). Epigenetic feedback and stochastic partitioning during cell division can drive resistance to EMT. Oncotarget 11, 2611–2624.

Jolly, MK, Preca, B-T, Tripathi, SC, Jia, D, George, JT, Hanash, SM, Brabletz, T, Stemmler, MP, Maurer, J, and Levine, H (2018). Interconnected feedback loops among ESRP1, HAS2, and CD44 regulate epithelial-mesenchymal plasticity in cancer. APL Bioeng 2, 031908.

Josefowicz, SZ (2013). Regulators of chromatin state and transcription in CD4 T-cell polarization. Immunology 139, 299–308.

Kaiko, GE, Horvat, JC, Beagley, KW, and Hansbro, PM (2008). Immunological decision-making: How does the immune system decide to mount a helper T-cell response? Immunology 123, 326–338.

Lee, S, Kim, J, Min, H, and Seong, RH (2020). RORγt-driven TH17 Cell Differentiation Requires Epigenetic Control by the Swi/Snf Chromatin Remodeling Complex. IScience 23, 101106.

Liu, C, Yang, H, Shi, W, Wang, T, and Ruan, Q (2018). MicroRNA-mediated regulation of T helper type 17/regulatory T-cell balance in autoimmune disease. Immunology 155, 427–434.

Martinez-Sanchez, ME, Huerta, L, Alvarez-Buylla, ER, and Luján, CV (2018). Role of cytokine combinations on CD4+ T cell differentiation, partial polarization, and plasticity: Continuous network modeling approach. Front Physiol 9, 1–14.

Messi, M, Giacchetto, I, Nagata, K, Lanzavecchia, A, Natoli, G, and Sallusto, F (2003). Memory and flexibility of cytokine gene expression as separable properties of human TH1 and TH2 lymphocytes. Nat Immunol 4, 78–86.

Miyamoto, T, Furusawa, C, and Kaneko, K (2015). Pluripotency, Differentiation, and Reprogramming: A Gene Expression Dynamics Model with Epigenetic Feedback Regulation. PLoS Comput Biol 11, e1004476.

Pedicini, M, Barrenäs, F, Clancy, T, Castiglione, F, Hovig, E, Kanduri, K, Santoni, D, and Benson, M (2010). Combining network modeling and gene expression microarray analysis to explore the dynamics of Th1 and Th2 cell regulation. PLoS Comput Biol 6, e1001032.

Peine, M, Rausch, S, Helmstetter, C, Fröhlich, A, Hegazy, AN, Kühl, AA, Grevelding, CG, Höfer, T, Hartmann, S, and Löhning, M (2013). Stable T-bet+GATA-3+ Th1/Th2 Hybrid Cells Arise In Vivo, Can

Develop Directly from Naive Precursors, and Limit Immunopathologic Inflammation. PLoS Biol 11, e1001633.

Pillai, M, and Jolly, MK (2021). Systems-level network modeling deciphers the master regulators of phenotypic plasticity and heterogeneity in melanoma. IScience 24, 103111.

Puniya, BL, Todd, RG, Mohammed, A, Brown, DM, Barberis, M, and Helikar, T (2018). A mechanistic computational model reveals that plasticity of CD4+ T cell differentiation is a function of cytokine composition and dosage. Front Physiol 9, 1–18.

Radens, CB, Blake, D, Jewell, P, Barash, Y, and Lynch, KW (2021). Meta-Analysis of Transcriptomic Variation in T cell Populations Reveals Novel Signatures of Gene Expression and Splicing. RNA 26, 1320–1333.

Sanders, VM (2006). Epigenetic regulation of Th1 and Th2 cell development. Brain Behav Immun 20, 317–324.

Sarkar, S, Sinha, SK, Levine, H, Jolly, MK, and Dutta, PS (2019). Anticipating critical transitions in epithelial-hybrid-mesenchymal cell-fate determination. Proc Natl Acad Sci U S A 116.

Serresi, M, Kertalli, S, Li, L, Schmitt, MJ, Dramaretska, Y, Wierikx, J, Hulsman, D, and Gargiulo, G (2021). Functional antagonism of chromatin modulators regulates epithelial-mesenchymal transition. Sci Adv 7, eabd7974.

Stadhouders, R, Lubberts, E, and Hendriks, RW (2018). A cellular and molecular view of T helper 17 cell plasticity in autoimmunity. J Autoimmun 87, 1–15.

Stark, JM, Tibbitt, CA, and Coquet, JM (2019). The Metabolic Requirements of Th2 Cell Differentiation. Front Immunol 10, 2318.

Suelves, M, Carrio, E, Nunez-Alvarez, Y, and Peinado, MA (2016). DNA methylation dynamics in cellular commitment and differentiation. Brief Funct Genomics 15, 443–453.

Tortola, L, Jacobs, A, Pohlmeier, L, Obermair, FJ, Ampenberger, F, Bodenmiller, B, and Kopf, M (2020). High-Dimensional T Helper Cell Profiling Reveals a Broad Diversity of Stably Committed Effector States and Uncovers Interlineage Relationships. Immunity 53, 597-613.e6.

Tripathi, S, Levine, H, and Jolly, MK (2020). The Physics of Cellular Decision-Making during Epithelial-Mesenchymal Transition. Annu Rev Biophys 49, 1–18.

Wei, G et al. (2009). Global Mapping of H3K4me3 and H3K27me3 Reveals Specificity and Plasticity in Lineage Fate Determination of Differentiating CD4+ T Cells. Immunity 30, 155–167.

Wilson, CB, Rowell, E, and Sekimata, M (2009). Epigenetic control of T-helper-cell differentiation. Nat Rev Immunol 9, 91–105.

Xhangholi, I, Dura, B, Lee, G, Kim, D, Xiao, Y, and Fan, R (2019). Single-cell Analysis of CAR-T Cell Activation Reveals A Mixed TH1/TH2 Response Independent of Differentiation. Genomics Proteomics Bioinformatics 17, 129–139.

Zhao, W, Qiao, L, Yan, S, Nie, Q, and Zhang, L (2021). Mathematical modeling of histone modifications reveals the formation mechanism and function of bivalent chromatin. IScience 24, 102732.

Zhou, JX, and Huang, S (2011). Understanding gene circuits at cell-fate branch points for rational cell reprogramming. Trends Genet 27, 55–62.